Published in final edited form as:
J Neurophysiol. 2003 July ; 90(1): 218–225. doi:10.1152/jn.01025.2002.

Properties of Exocytotic Response in Vertebrate Photoreceptors

M. Kreft[1,2,*], **D. Križaj**[3,*], **S. Grilc**[1], and **R. Zorec**[1,2]

[1] Laboratory Neuroendocrinology-Molecular Cell Physiology, Institute of Pathophysiology, Medical Faculty, Zalos ka 4

[2] Celica Biomedical Sciences Center, Stegne 21, 1000 Ljubljana, Slovenia

[3] Departments of Ophthalmology and Physiology, University of California School of Medicine, San Francisco, California 94143-0730

Abstract

Synaptic transmission at the photoreceptor synapse is characterized by continuous release of glutamate in darkness. Release is regulated by the intracellular calcium concentration ($[Ca^{2+}]_i$). We here examined the physiological properties of exocytosis in tiger salamander (*Ambystoma tigrinum*) retinal rods and cones. Patch-clamp capacitance measurements were used to monitor exocytosis elicited by a rapid and uniform increase in $[Ca^{2+}]_i$ by photolysis of the caged Ca^{2+} compound NP-EGTA. The amplitude of flash-induced increases in membrane capacitance (C_m) varied monotonically with $[Ca^{2+}]_i$ beyond approximately 15 μM. The following two types of kinetic responses in C_m were recorded in both rods and cones: *1*) a single exponential rise (39% of cells) or *2*) a double-exponential rise (61%). Average rate constants of rapid and slow exocytotic responses were 420 ± 168 and 7.85 ± 5.02 s^{-1}, respectively. The rate constant for the single exponential exocytotic response was 17.5 ± 12.4 s^{-1}, not significantly different from that of the slow exocytotic response. Beyond the threshold $[Ca^{2+}]_i$ of approximately 15 μM, the average amplitude of rapid, slow, and single C_m response were 0.84 ± 0.35, 0.82 ± 0.20, and 0.70 ± 0.23 pF, respectively. Antibodies against synaptotagmin I, a vesicle protein associated with fast exocytosis, strongly stained the synaptic terminal of isolated photoreceptors, suggesting the presence of fusion-competent vesicles. Our results confirm that photoreceptors possess a large rapidly releasable pool activated by a low-affinity Ca^{2+} sensor whose kinetic and calcium-dependent properties are similar to those reported in retinal bipolar cells and cochlear hair cells.

INTRODUCTION

Light responses of retinal receptors and bipolar cells are characterized by sustained and graded voltage changes on the time scale of hundreds of milliseconds to seconds (Tomita 1986). This is in contrast with the millisecond time scale of action potentials which trigger rapid and transient exocytotic events in “conventional” neurons. Consequently, photoreceptor and bipolar synapses are designed to optimize high rates of sustained neurotransmitter release (reviewed in Juusola et al. 1996; Krizaj and Copenhagen 2002; von Gersdorff 2001). Analysis of molecular components of exocytosis at graded synapses in the retina revealed that they share many features in common with conventional synapses (von Kriegstein et al. 1999). However, in contrast to conventional synapses, graded synapses can maintain transmitter release for hours, suggesting that they possess highly efficient mechanisms for vesicle retrieval and/or a virtually limitless supply of releasable vesicles.

Address for reprint requests: R. Zorec, Celica Biomedical Sciences Center, Stegne 21, 1000 Ljubljana, Slovenia (Robert.Zorec@mf.uni-lj.si).

*M. Kreft and D. Križaj contributed equally to this paper.

Ultrastructural analysis of synaptic terminals of graded neurons such as photoreceptors and bipolar cells reveals an elaborate organization dominated by the synaptic ribbon, a laminar structure whose function is thought to be fast delivery of vesicles to the active zone (Gray and Pease 1971; von Gersdorff 2001). A similar structure, the “dense body,” is found in the synaptic region of the hair cell (e.g., Safieddine and Wenthold 1999). It has been suggested that these structures gate both rapid and sustained phases of neurotransmitter release and thus provide photoreceptors, bipolar cells, and hair cells with the ability to sustain vesicle release rates ten to hundreds of times higher compared with those at conventional synapses (Gray and Pease 1971; Parsons et al. 1994; Rao-Mirotznik et al. 1995; Rieke and Schwartz 1996; von Gersdorff 2001).

Exocytosis at most ribbon synapses is characterized by at least two kinetically distinct components—a fast component ranging from several milliseconds to several tens of milliseconds and a slow component in the order of several hundred milliseconds (Beutner et al. 2001; Gomis et al. 1999; Moser and Beutner 2000; Neves and Lagnado 1999; Parsons et al. 1994; Rouze and Schwartz 1998; Sakaba et al. 1997; von Gersdorff et al. 1996). Two models have been proposed to account for the fast and the slow kinetic components of vesicle release at ribbon synapses. The “sequential model” proposes a sequential activation of separate vesicle pools. According to this model, a “rapidly releasable pool” of fusion-ready vesicles is recruited from several rows of vesicles tethered to the ribbon, whereas a much larger “reserve pool” may be recruited from the population of nontethered vesicles within the terminal (Neves and Lagnado 1999; Sakaba et al. 1997; von Gersdorff et al. 1996). The sequential model is supported by the observations in terminals from teleost bipolar cells in which the rapidly releasable pool was found to deplete before activation of the reserve pool (Gomis et al. 1999; Sakaba et al. 1997; von Gersdorff et al. 1996), and in amphibian hair cells, where prolonged rapid exocytosis involves vesicles from a larger pool than could be in close proximity to the plasma membrane at active zones (Parsons et al. 1994). Alternatively, the “parallel model” suggests exocytosis occurs in parallel from spatially separated vesicle pools. Therefore, according to this model, exocytosis need not occur solely from the vesicles docked at the ribbon but may occur at active sites elsewhere within the synaptic terminal. Evidence suggestive of parallel exocytosis in retinal bipolar cell terminals has been recently provided by direct measurements of vesicle dynamics using evanescent field microscopy. These experiments showed that exocytosis of fusion-competent vesicles can occur from sites distal to the synaptic ribbon (Zenisek et al. 2000). Parallel exocytosis has been documented in many other cell types, including PC12 cells (Kasai et al. 1996), melanotrophs (Kreft et al. 2003; Poberaj et al. 2002; Rupnik et al. 2000), chromaffin cells (Voets 2000), and pancreatic β cells (Takahashi et al. 1997; reviewed in Kasai 1999).

Ribbon synapses are characterized by their ability to sustain prolonged periods of elevated $[Ca^{2+}]_i$, which controls the graded release of the neurotransmitter (Sakaba et al. 1997; Tachibana et al. 1993). Paradoxically, the Ca^{2+} dependence of release seems to be different between different classes of ribbon synapses in the retina: whereas several release mechanisms are thought to operate in bipolar cells, each at different optimal $[Ca^{2+}]_i$, rod photoreceptors are thought to operate mostly at $[Ca^{2+}]_i < 2\ \mu M$ (Lagnado et al. 1996; Rieke and Schwartz 1996; Rouze and Schwartz 1998; von Gersdorff and Matthews 1999). Flash photolysis experiments in bipolar cells suggest that the $[Ca^{2+}]_i$ threshold for fast exocytosis is high, above approximately 20–50 μM (Heidelberger et al. 1994; Mennerick and Matthews 1996; von Gersdorff et al. 1996). Bipolar cells thus possess a large rapidly releasable pool activated by a low-affinity Ca^{2+} sensor (Heidelberger et al. 1994; but see Rouze and Schwartz 1998). Optical measurements using lipophilic dyes suggest that, in addition to the high-threshold exocytosis, sustained vesicle cycling in bipolar cells may also occur at submicromolar $[Ca^{2+}]_i$ (Gomis et al. 1999; Lagnado et al. 1996; Rouze and Schwartz 1998).

Bipolar ribbon synapses may thus possess both high- and low-affinity sensors for exocytosis.

In contrast to bipolar cells, exocytosis in photoreceptors has not been studied in great detail and the properties of kinetics of release and Ca^{2+} dependence of secretion in rods and cones are not well understood. The secretion responses in rod photoreceptors were shown to be sustained and proportional to changes in $[Ca^{2+}]_i$ (Rieke and Schwartz 1996). Moreover, rod photoreceptors were reported to only operate at relatively low (0.5 to 2.0 μM) $[Ca^{2+}]_i$ (Rieke and Schwartz 1996). These findings led to the suggestion that transmitter release in rod photoreceptors is mainly controlled by residual $[Ca^{2+}]_i$ and operates at high affinity for Ca^{2+}. It can be predicted, therefore, that exocytosis in photoreceptors follows changes in global $[Ca^{2+}]_i$ rather than changes within Ca^{2+} microdomains. The discrepancy in kinetics and Ca^{2+} affinity of vesicle release between photoreceptors and bipolar cells suggests that the synaptic transmission at the photoreceptor synapse is fundamentally different from that of the bipolar synapse (von Gersdorff and Matthews 1999). However, in the original study (Rieke and Schwartz 1996) the cells were not studied with the same protocol applied previously to bipolar cells (Heidelberger et al. 1994). It is therefore not clear whether photoreceptors only possess high Ca^{2+} affinity release. To test this hypothesis experimentally, we re-investigated the kinetics and Ca^{2+} dependence of exocytosis in photoreceptors using a combination of flash photolysis of caged Ca^{2+} and capacitance measurements to evoke and monitor changes in $[Ca^{2+}]_i$ and vesicle cycling, respectively. Our methods were designed to mimic those used in the original studies on retinal bipolar cells (e.g., Heidelberger et al. 1994).

We found that kinetics of exocytosis at the photoreceptor synaptic terminal are similar to that reported for retinal bipolar cells, whereas Ca^{2+}-sensitivity threshold is slightly lower, at approximately 15 μM. In a majority of cells tested we found both fast and slow components of exocytosis. Our results therefore suggest that exocytosis in photoreceptors is relatively similar to that observed in bipolar cells with respect to kinetics of vesicle release and its Ca^{2+} dependence.

METHODS

Cell preparation

Rod and cone photoreceptor cells from tiger salamander (*Ambystoma tigrinum*) retina were acutely dissociated by enzymatic dissociation and mechanical trituration, as previously described (Krizaj and Copenhagen 1998). Larval-stage tiger salamander retinas were dissected and incubated on a shaker in calcium-depleted saline with papain (7 U/ml; Worthington, Freehold, NJ) for 25 min and triturated with a BSA-coated Pasteur pipette. The outer segments of many rods were shorn during the isolation procedure, resulting in the absence of the dark current and hyperpolarization of their membrane potentials. Cell isolation was performed at room light; therefore, all cells that kept their outer segments were completely light adapted. Cells were kept at 4°C in 80% L-15 medium supplemented with 10 mM HEPES, 20 mM glucose, 1 mM pyruvic acid, 1 mg/ml bovine serum albumin (BSA), and 1 μl/ml liquid media supplement containing transferrin and selenium (Sigma, St. Louis, MO). Cells were seeded onto acid-cleaned glass coverslips coated with IgG and/or IgM (Jackson ImmunoResearch, West Grove, PA) and the Sal-1 antibody (a kind gift from Dr. Peter MacLeish; MacLeish et al. 1983).

Immunocytochemistry and confocal microscopy

For immunocytochemical detection of synaptotagmin I, enzymatically dissociated photoreceptor cells were washed with phosphate-buffered saline (PBS) and then fixed for 15

min in 4% paraformaldehyde in PBS. Cells were kept in fixative containing 0.1% of Triton X-100 for 10 min and washed four times with PBS. Nonspecific staining was reduced by incubating cells in 3% BSA and 10% normal goat serum in PBS. Cells were then incubated with primary antibodies for 2 h at 37°C. We used mouse anti-synaptotagmin I monoclonal antibody (Leveque et al. 1992; Takahashi et al. 1991) diluted 1:2,000 in PBS containing 3% BSA. Cells were then washed and incubated in PBS containing Alexafluor 546 labeled anti-mouse secondary antibodies (1:2,000; Molecular Probes, Oregon, USA) and 3% BSA for 45 min. Light Antifade Kit (Molecular Probes) was used for mounting. Cells were monitored with a confocal microscope (Zeiss, LSM 510, objective ×63, NA = 1.4). Alexafluor 546 was excited with a He/Ne (543 nm) laser. Emission signals were filtered using a LP 560-nm filter.

Membrane capacitance measurements

Compensated membrane capacitance (C_m) measurements were used (Lindau and Neher 1988; Neher and Marty 1982; Zorec et al. 1991), employing a SWAM IIB patch-clamp/lock-in amplifier (Celica, Ljubljana, Slovenia), operating at 1.6 kHz lock-in frequency.

On establishment of the whole-cell configuration, C_m and G_a (access conductance) were compensated by C_{slow} and G_a compensation controls. A sine voltage of 314 mV (peak-to-peak) was applied. The phase-angle setting was determined by a 1-pF calibration pulse and by monitoring the projection of this pulse from the C (signal proportional to C_m) to the G output of the lock-in amplifier (asterisk in Fig. 2). These two signals were stored unfiltered (C-DAT4 recorder, Cygnus, USA) for off-line analysis. Simultaneously, we recorded filtered (300 Hz, 4-pole Bessel) C and G signals, the fluorescence intensity from a C660 photon counter (Thorn EMI, UK), and membrane current (0–10 Hz, low-pass). PhoCal program (LSR, UK) was used to acquire signals every 5 ms. For high temporal resolution measurements of C_m, the records on DAT were played back and a 10-s epoch of the signal enveloping each flash was digitized at 50 kHz using a computer disk recorder (CDR) program (J. Dempster, Strathclyde Electrophysiology Software). Signals were digitally filtered at 1 kHz (2-way 150th order FIR filter, Math Works MATLAB) and resampled at 10 kHz. The pipette solution contained the following (in mM): 88 KCl, 8 TEACl, 32 KOH/HEPES, 1.6 Na_2ATP, 1.6 $MgCl_2$, 4.0 K_4-NP-EGTA, 2.9 $CaCl_2$, 0.5 furaptra, pH 7.6. The bath contained the following (in mM): 105.4 NaCl, 4 KCl, 1.6 $MgCl_2$, 0.4 NaH_2PO_4, 4 $NaHCO_3$, 8 Na HEPES, 8 D-glucose, 1.4 $CaCl_2$, pH 7.6.

All recordings were made at room temperature. The salts were obtained from Sigma. Cells were voltage clamped at a holding potential of −50 mV. The average cell capacitance was 13.2 ± 0.83 pF (n = 23; mean ± SE). Recordings were made with pipette resistances between 1 and 4 MΩ (measured in KCl-rich solution), giving access conductance of more than 80 nS (117 ± 14.2 nS; mean ± SE). The pipette and bath solutions were of similar osmolarity (within 5%) measured by freezing point depression (Camlab, Cambridge, UK). Na_2ATP was included in the pipette solution since it has a major role in preparing synaptic vesicles for fusion (Heidelberger 1998). Under our experimental conditions, endocytosis was not regularly observed, probably as a result of the washout of a critical component (e.g., Parsons et al. 1994). We therefore focused on the exocytotic component. Moreover, although several UV flashes were applied during any given experiment, the second flash always elicited a smaller capacitance jump, presumably because of vesicle depletion and blocked endocytosis. Only the first exocytotic responses to photolysis flashes were analyzed in this study.

Flash photolysis and $[Ca^{2+}]_i$ measurements

The Ca^{2+} cage NP-EGTA (Molecular Probes) was used to elevate $[Ca^{2+}]_i$ by flash photolysis (Ellis-Davies and Kaplan 1994). A 1-ms UV flash from an Xe arc flash lamp

(Rapp and Güth 1988) was delivered to cells through a ×40 fluor oil immersion objective of a Nikon Diaphot microscope. The same optical pathway as in flash photolysis was used to illuminate the fluorescent [Ca^{2+}] indicator furaptra (Molecular Probes). A combination of two dichroic mirrors was used. The first one was a 390-nm dichroic positioned at 45°, which passed through the 420-nm light for furaptra excitation from a Xe arc lamp and reflected the light below 390 nm for NP-EGTA flash photolysis from a Xe arc flash lamp. The second 430-nm dichroic reflected both lights through the objective to the cell under experiment and allowed only furaptra fluorescent light to pass back to the photomultiplier through a 510-nm barrier filter. $[Ca^{2+}]_i$ measurements were performed as described by Carter and Ogden (1994). The equation used in calculation is

$$[Ca^{2+}]_i = K_d \frac{F - F_{min}}{F_{max} - F}$$

where F_{max} is the autofluorescence in the cell-attached configuration, F_{min} is the fluorescence in a resting whole-cell recording, and F is fluorescence during the flash. K_d for furaptra is 25 μM. K_d for Ca^{2+}-NP-EGTA complex before photolysis is 80 nM. $[Ca^{2+}]_i$ in unstimulated cells was measured in other experiments using the high-affinity dye fura-2 and was shown to be approximately 20–100 nM (Krizaj and Copenhagen 1998; Krizaj et al. 2003).

RESULTS

Ca^{2+}-dependent increase in C_m

We photolyzed the caged Ca^{2+} compound NP-EGTA to rapidly increase cytosolic [Ca^{2+}] in a spatially uniform manner in the photoreceptor terminals (Neher and Zucker 1993). Only cells with well-preserved morphology of the synaptic terminal were examined physiologically (Fig. 1). In several cells, the synaptic terminals were resorbed following isolation and these cells were avoided in single-cell capacitance measurements described in this study.

Figure 2 shows a C_m response of a rod photoreceptor to a flash of UV light. The flash discharge increased $[Ca^{2+}]_i$ to 56 μM in <10 ms (the time resolution limit of fluorescence recording system; Fig. 2, arrow), whereupon $[Ca^{2+}]_i$ returned to the baseline with a time constant of around 5 s. Following flash photolysis and $[Ca^{2+}]_i$ increase within the terminal, an exponential increase in C_m to the final amplitude of 1.86 pF (labeled *A* in Fig. 2) was observed. A small change in the real part of admittance signal (G) was observed following flash photolysis (G, Fig. 2). The change in G was transient and was not correlated to the increase in C_m. It may be attributed to calcium-induced activation of ion channels (Maricq and Korenbrot 1988;Moriondo et al. 2001) or/and may reflect fusion pore conductance of many synchronously exocytosed vesicles (Lindau 1991). The time course of the C_m response in this cell was well described by a single exponential function with a time constant of 1.19 s. Assuming a vesicle diameter of 30 nm and assuming the specific membrane capacitance of 8 fF/μm^2, a single-vesicle capacitance is approximately 23 aF (von Gersdorff et al. 1996;Zenisek et al. 2000). Therefore the amplitude of 1.86 pF corresponds to the fusion of approximately 80,000 vesicles with the membrane of the photoreceptor. The number of exocytosed vesicles is at least one order of magnitude larger than the pool of rapidly releasable vesicles docked at approximately 60 ribbons in the teleost Mb1 bipolar cell (von Gersdorff et al. 1996;von Gersdorff and Matthews 1999).

We measured the maximal amplitude of C_m elevation after stimulation with flash photolysis of NP-EGTA. Only C_m responses to the first photolysis flash were analyzed in any cell (see METHODS). The evoked maximal $[Ca^{2+}]_i$ varied between 5 and 60 μM. The C_m amplitude exhibited a sigmoidal dependence on $[Ca^{2+}]_i$ with the half-maximal response at approximately 30 μM for both rods and cones (Fig. 3). The threshold of $[Ca^{2+}]_i$ at which exocytosis was observed was at 10–15 μM $[Ca^{2+}]_i$, whereas maximal C_m amplitude was observed at approximately 50 μM $[Ca^{2+}]_i$.

Two kinetic components of flash-induced C_m changes in photoreceptors

To quantify the kinetics of C_m responses, both single- and double-exponential functions were fitted to the rising phase of each C_m trace. Capacitance responses were best described by either a single exponential (39% of 18 photoreceptors studied) or a double-exponential time course to the peak (61%). The goodness of fit was evaluated by squared correlation coefficients (coefficients of determination) and by visual inspection. The two types of responses are illustrated in Fig. 4 for two cones. The response of the cell depicted in Fig. 4*A* was best fit with a single exponential function with a time constant of 1.19 s. The majority of cells exhibited two visually distinct time courses. These were best fit with a double exponential function. One such cell, shown in Fig. 4*B*, had a time constant for the rapid phase of the C_m response of 94.1 ms, whereas the time constant for the slow phase was 1.77 s. The range of time constants for the rapid exocytic response was from 0.5 to 135.0 ms and for the slow exocytic response in the biphasic C_m traces was from 0.02 to 8.40 s. No significant differences in the kinetics of C_m responses were observed between rods and cones (Fig. 3). The Ca^{2+} dependence of rate constants appeared as a step-like function, with an all-or-none response beyond the threshold $[Ca^{2+}]_i$ of 10–15 μM (Fig. 5*C*). The slopes of the linear fit of logarithmized rapid, slow, and single time constants versus $[Ca^{2+}]_i$ did not differ significantly from zero.

Figure 5*A* shows the estimated amplitudes of exponential functions obtained in fitting monophasic and biphasic exponential functions to the experimentally recorded flash-evoked changes in C_m. Mean amplitudes of rapid and slow components of double-exponential exocytotic responses were not significantly different (0.84 ± 0.35 and 0.82 ± 0.20 pF, respectively; n = 11 cells, mean ± SE). Likewise, the mean amplitude of the single exponential response in C_m was not significantly different (0.70 ± 0.23 pF; n = 7) from either the mean rapid or the mean slow components. The mean rate constants of single- or double-exponential curves in C_m are graphed in Fig. 5*B*. Mean rate constant of the rapid exocytosis was 53 times faster than the mean rate constant for the slow component of C_m response (420 ± 168 and 7.85 ± 5.02 s^{-1}, respectively). The mean rate constant of single exponential exocytotic response in C_m (17.5 ± 12.4 s^{-1}) was not significantly different from the mean rate constant of the slow component of double-exponential exocytotic response. Corresponding mean time constants for rapid, slow, and single exponential response are 24.7 ± 13.7 ms, 1.59 ± 0.75 s, and 0.51 ± 0.17 s, respectively. These results indicate that the majority of cells responded to stimulation with a biphasic exocytotic response. This may indicate that in these photoreceptor cells two kinetically distinct readily releasable pools of vesicles coexist.

Synaptotagmin I is localized to vesicles in the synaptic terminal of photoreceptors

Synaptotagmin I is a synaptic vesicle protein suggested to be involved in neurotransmitter release at conventional synapses (Geppert et al. 1994; Schiavo et al. 1997). This ubiquitous vesicle protein has a relatively low affinity for Ca^{2+} (Davis et al. 1999) and is thought to support fast, “synchronous” transmitter release (Geppert et al. 1994; Goda and Stevens 1994; Kreft et al. 2003; Schiavo et al. 1997; Voets et al. 2001). Expression of synaptotagmin

I in salamander rods and cones provides additional confirmatory evidence for our observation that these cells are capable of fast exocytosis.

Figure 1 (*left*) shows a Nomarski image of an isolated rod photoreceptor. The cell consists of the inner segment with a cell body and a prominent synaptic terminal. The outer segment was shorn from this cell during the dissociation procedure. The cell was immunolabeled with the antibody against synaptotagmin I. As shown in Fig. 1 (*right*), synaptotagmin I is selectively expressed in the synaptic terminal, consistent with a large pool of vesicles being preserved under our experimental conditions. Similar results were obtained with SV2, another marker for vesicles within photoreceptor terminals (data not shown). This finding indicates that rapid exocytosis, observed in salamander photoreceptors, may be subserved by molecular machinery similar to that found in conventional synapses. Moreover, the observation of robust presence of synaptotagmin- and SV2-positive terminals is consistent with our physiological measurements of secretory function of the photoreceptor terminal in dissociated cells.

DISCUSSION

The aim of our work was to examine the kinetics and Ca^{2+} dependence of exocytosis in salamander photoreceptors. Previously, release in photoreceptors was shown to be regulated by low micromolar $[Ca^{2+}]_i$ and no kinetically distinct components of secretion were observed (Rieke and Schwartz 1996). These findings (Rieke and Schwartz 1996) suggested that transmitter release from rod photoreceptors is fundamentally different from that at the bipolar cell terminal (Heidelberger et al. 1994; Sakaba et al. 1997).

In our experiments, measurements of C_m combined with flash photolysis of caged Ca^{2+} revealed that the majority of cells (61%) respond to flash photolysis with an exocytotic response consisting of two kinetic components (Fig. 4). These two components were observed in both rods and cones (Fig. 3). The fast response was characterized by a mean time constant of 24 ms, ranging from 0.5 to 135 ms. The vesicles comprising the fast exocytotic pool are likely to include those already docked at active sites and tethered to the ribbon, as shown in studies with bipolar cells (Heidelberger et al. 1994;Mennerick and Matthews 1996;Neves and Lagnado 1999;Sakaba et al. 1997;von Gersdorff et al. 1996). The capacitance jump corresponding to the rapidly releasable pool in teleost bipolar cells is approximately 150 fF, whereas the mean size of the fast component in salamander photoreceptors was 840 fF, corresponding to release of approximately 34,000 vesicles. This is similar to what has been observed in mammalian cochlear hair cells (approximately 40,000 vesicles; Beutner et al. 2001) but is much higher than the estimates in bipolar cells (about 6,000 vesicles; von Gersdorff et al. 1996). A photolysis flash could trigger exocytosis of several tens of thousands of vesicles in both fast and slow components, suggesting that the exocytosis draws vesicles from a larger pool than could exist in close proximity to the synaptic ribbon. For example, a ribbon in a mammalian rod may tether about 770 vesicles (Rao-Mirotznik et al. 1995). This would correspond to about 18 fF. Thus even if taking into account that salamander ribbons can accommodate a larger number of vesicles than mammalian rods and that a single salamander rod terminal may possess multiple ribbons, it is unlikely that the capacitance jump observed during the fast exocytic response derives solely from the pool of vesicles tethered to the ribbon and docked at the active site. The amplitudes of exocytic responses in rods and cones were not significantly different (not shown).

We also found that a smaller percentage of examined cells lacked the faster component of exocytosis. It is possible that cells with a single exocytotic (slow) phase lack the rapid phase due to the cell isolation procedure. Whatever the cause underlying the differences between

the slow and fast response, the absence of the latter during the slow exocytotic response argues against the model in which the rapid and slow components in photoreceptor C_m occur by sequential coupling of two pools of vesicles (Neher and Zucker 1993; Thomas et al. 1993; Xu et al. 1998). As is the case with the fast pool, the size of the slow sustained pool is likely to be larger than the combined surface area of the vesicles tethered to the ribbon, suggesting an additional contribution from fusion competent vesicles distal to the ribbon. Zenisek et al. (2000) reported that vesicle exocytosis in fish bipolar cells may occur at sites away from the active zone and thus ribbons may not be absolutely required for docking and exocytosis at graded synapses. Similarly, electron microscopic analysis of salamander photoreceptor terminals suggests that exocytosis may occur at the ribbons as well as at basal junctions, specializations of the synaptic terminal which contact postsynaptic processes in the absence of associated synaptic ribbons (Lasansky 1973). Several kinds of basal junctions have been observed in salamander rods and cones (Lasansky 1973); likewise, recent studies have shown that synaptic vesicles in frog saccular cells may be docked at the presynaptic membrane at some distance from the active zones (Lenzi et al. 1999). A parsimonious explanation for the two phases observed in salamander photoreceptors may be that they occur via parallel vesicle release processes at ribbon and at extra-ribbon sites. Changes in C_m may also reflect fusion of subcellular compartments other than vesicles (for example, lysosomes, endosomes, granules, etc.). Using capacitance measurements on single cells, we cannot distinguish the relative contributions of these compartments to the total C_m increase. Furthermore, large changes in C_m may be due to multivesicular exocytosis.

If photoreceptors operated only using asynchronous release, they would be expected to lack synaptotagmin I, known to be a major vesicle component underlying fast synchronous exocytosis (Geppert et al. 1994). Synaptotagmin I binds multiple Ca^{2+} ions (Fernandez-Chacon et al. 2001; Ubach et al. 1998), has a relatively low affinity for Ca^{2+} (Davis et al. 1999) and is essential for fast, Ca^{2+}-triggered exocytosis in conventional synapses (Geppert et al. 1994). We therefore examined the subcellular distribution of synaptotagmin I in photoreceptors, using immunocytochemistry and confocal microscopy. The anti-synaptotagmin I antibody strongly labeled synaptic terminals in both rods and cones, consistent with the presence of fast, synchronous vesicle release in these cells. The expression of synaptotagmin I in salamander photoreceptors is consistent with the recent report by von Kriegstein et al. (1999) in which a prominent synaptotagmin I signal was observed in the outer retina of cattle and supports the idea that conventional and ribbon synapses share many molecular components of the exocytotic machine (Ullrich and Sudhof 1994; von Kriegstein et al. 1999). For example, other elements of the soluble *N*-ethylmaleimide-sensitive factor attachment protein receptor complex found in photoreceptors include synaptosome-associated protein of 25 kDa and synaptobrevin (Sherry et al. 2001; von Kriegstein et al. 1999).

$[Ca^{2+}]_i$ above 15 μM was required to trigger secretion in photoreceptors with a half-saturating response at approximately 30 μM (Fig. 3). This Ca^{2+} dependence of release is similar to that previously reported in retinal bipolar cells. Dialysis of bipolar cell terminals with solutions containing buffered amounts of elevated calcium concentration and flash photolysis experiments demonstrated that exocytosis in these cells requires $[Ca^{2+}]_i$ above approximately 20–50 μM (Heidelberger et al. 1994;von Gersdorff and Matthews 1994). Our finding therefore suggests that exocytosis in photoreceptors may be triggered within microdomains of high-calcium concentration expected near open calcium channels (Chad and Eckert 1984;Neher 1998) rather than by the relatively low $[Ca^{2+}]_i$ measured in cells at dark potentials (approximately 300 nM at approximately −40 mV; Krizaj et al. 1999). This view is also supported by the observation that a high density of voltage-gated calcium channels is often found at the active zone close to the synaptic ribbon (Morgans 2001;Morgans et al. 1998;Nachman-Clewner et al. 1999;Raviola and Raviola 1982;

reviewed by Lenzi and von Gersdorff 2001). The technique we used is not sensitive enough to resolve fusion of single synaptic vesicles (e.g., Kreft and Zorec 1997). Similarly, exocytotic rates of ≤2,000 vesicles/s measured in bipolar cells using optical dyes (Lagnado et al. 1996;Rouze and Schwartz 1998) may have been missed during capacitance measurements by Heidelberger et al. (1994) (cf. Beutner et al. 2001).

Rieke and Schwartz (1996) reported that photoreceptor exocytosis operates at high (0.5–1.0 μM) Ca^{2+} affinity. We do not know the reason for the observed differences in our study and in the work by Rieke and Schwartz (1996), but different experimental approaches may account for this. For example, Rieke and Schwartz (1996) adjusted the intensity and duration of the photolysis flash so that the time course of $[Ca^{2+}]_i$ changes approximated the cell voltage during the light response. The long rise times (on the order of seconds) and long decay times of $[Ca^{2+}]_i$ following flash photolysis may have contributed to favoring a component of release with high Ca^{2+} affinity. However, the time course of Ca^{2+} decay was much slower from the time course expected from the synaptic terminal (Morgans et al. 1998; D. Krizaj, unpublished observations) and known properties of synaptic transfer at the photoreceptor synapse (Schnapf and Copenhagen 1982). It is possible that photoreceptors possess both fast release and slow asynchronous release at high and low Ca^{2+} affinity. Synaptotagmin I may be the Ca^{2+} sensor required for the fast release, whereas slow release may be supported by at present unknown proteins or different isoforms of synaptotagmins. More than 12 isoforms of synaptotagmins are present in the brain in addition to synaptotagmin I and may participate in regulating secretion at higher Ca^{2+} affinities (Sugita et al. 2002). For example, synaptotagmins IV, VI, VII, VIII, and IX have been recently identified at the “ribbon” synapse of the hair cell (Safieddine and Wenthold 1999).

In summary, our study revealed that at least two separate pools of secretory vesicles are present in rod and cone photoreceptors and that salamander photoreceptors possess a large pool of fusion-ready vesicles activated by a low-affinity Ca^{2+} sensor similar to the bipolar cells. Our results suggest that graded release in photoreceptors and bipolar cells may be regulated by similar molecular pathways.

Acknowledgments

We thank M. Seagar for the synaptotagmin I antibody and P. MacLeish for the Sal-1 antibody. We also thank R. Rentería and D. Copenhagen for helpful advice and critical reading of the manuscript.

This work was supported by Ministry of Education, Science, and Sport of the Republic of Slovenia Grant J3-2344-7421-00 to M. Kreft, National Eye Institute Grant EY-32918 to D. Križaj, Wheeler Center for Neurobiology of Addiction to D. Križaj, University of California San Francisco Academic Senate Individual Investigator Award to D. Križaj, P3 521 381 to R. Zorec, and the European Union Grant QLG3 2001–2004 to R. Zorec.

References

Beutner D, Voets T, Neher E, Moser T. Calcium dependence of exocytosis and endocytosis at the cochlear inner hair cell afferent synapse. Neuron 2001;29:681–690. [PubMed: 11301027]

Carter TD, Ogden D. Acetylcholine-stimulated changes of membrane potential and intracellular Ca^{2+} concentration recorded in endothelial cells *in situ* in the isolated rat aorta. Pfluegers Arch 1994;428:476–484. [PubMed: 7838669]

Chad JE, Eckert R. Calcium domains associated with individual channels can account for anomalous voltage relations of CA-dependent responses. Biophys J 1984;45:993–999. [PubMed: 6329349]

Davis AF, Bai J, Fasshauer D, Wolowick MJ, Lewis JL, Chapman ER. Kinetics of synaptotagmin responses to Ca^{2+} and assembly with the core SNARE complex onto membranes. Neuron 1999;24:363–376. [PubMed: 10571230]

Ellis-Davies GC, Kaplan JH. Nitrophenyl-EGTA, a photolabile chelator that selectively binds Ca^{2+} with high affinity and releases it rapidly upon photolysis. Proc Natl Acad Sci USA 1994;91:187–191. [PubMed: 8278362]

Fernandez-Chacon R, Konigstorfer A, Gerber SH, Garcia J, Matos MF, Stevens CF, Brose N, Rizo J, Rosenmund C, Südhof TC. Synaptotagmin I functions as a calcium regulator of release probability. Nature 2001;410:41–49. [PubMed: 11242035]

Geppert M, Bolshakov VY, Siegelbaum SA, Takei K, De Camilli P, Hammer RE, Sudhof TC. The role of Rab3A in neurotransmitter release. Nature 1994;369:493–497. [PubMed: 7911226]

Goda Y, Stevens CF. Two components of transmitter release at a central synapse. Proc Natl Acad Sci USA 1994;91:12942–12946. [PubMed: 7809151]

Gomis A, Burrone J, Lagnado L. Two actions of calcium regulate the supply of releasable vesicles at the ribbon synapse of retinal bipolar cells. J Neurosci 1999;19:6309–6317. [PubMed: 10414960]

Gray EG, Pease HL. On understanding the organisation of the retinal receptor synapses. Brain Res 1971;35:1–15. [PubMed: 5134225]

Heidelberger R. Adenosine triphosphate and the late steps in calcium-dependent exocytosis at a ribbon synapse. J Gen Physiol 1998;111:225–241. [PubMed: 9450941]

Heidelberger R, Heinemann C, Neher E, Matthews G. Calcium dependence of the rate of exocytosis in a synaptic terminal. Nature 1994;371:513–515. [PubMed: 7935764]

Juusola M, French AS, Uusitalo RO, Weckstrom M. Information processing by graded-potential transmission through tonically active synapses. Trends Neurosci 1996;19:292–297. [PubMed: 8799975]

Kasai H. Comparative biology of Ca^{2+}-dependent exocytosis: implications of kinetic diversity for secretory function. Trends Neurosci 1999;22:88–93. [PubMed: 10092049]

Kasai H, Takagi H, Ninomiya Y, Kishimoto T, Ito K, Yoshida A, Yoshioka T, Miyashita Y. Two components of exocytosis and endocytosis in phaeochromocytoma cells studied using caged Ca^{2+} compounds. J Physiol 1996;494:53–65. [PubMed: 8814606]

Kreft M, Zorec R. Cell-attached measurements of attofarad capacitance steps in rat melanotrophs. Pfluegers Arch 1997;434:212–214. [PubMed: 9136678]

Kreft M, Kuster V, Grilc S, Rupnik M, Milisav I, Zorec R. Synaptotagmin-I increases the probability of vesicle fusion at low [Ca^{2+}] in pituitary cells. Am J Physiol Cell Physiol 2003;284:C547–C554. [PubMed: 12388083]

Krizaj D, Copenhagen DR. Calcium regulation in photoreceptors. Front Biosci 2002;7:d2023–d2044. [PubMed: 12161344]

Krizaj D, Copenhagen DR. Compartmentalization of calcium extrusion mechanisms in the outer and inner segments of photoreceptors. Neuron 1998;21:249–256. [PubMed: 9697868]

Krizaj D, Bao JX, Schmitz Y, Witkovsky P, Copenhagen DR. Caffeine-sensitive calcium stores regulate synaptic transmission from retinal rod photoreceptors. J Neurosci 1999;19:7249–7261. [PubMed: 10460231]

Krizaj D, Lai FA, Copenhagen DR. Ryanodine stores and calcium regulation in the inner segments of salamander rods and cones. J Physiol 2003;547:761–774. [PubMed: 12562925]

Lagnado L, Gomis A, Job C. Continuous vesicle cycling in the synaptic terminal of retinal bipolar cells. Neuron 1996;17:957–967. [PubMed: 8938127]

Lasansky A. Organization of the outer synaptic layer in the retina of the larval tiger salamander. Philos Trans R Soc Lond B Biol Sci 1973;265:471–489. [PubMed: 4147132]

Lenzi D, Runyeon JW, Crum J, Ellisman MH, Roberts WM. Synaptic vesicle populations in saccular hair cells reconstructed by electron tomography. J Neurosci 1999;19:119–132. [PubMed: 9870944]

Lenzi D, von Gersdorff H. Structure suggests function: the case for synaptic ribbons as exocytotic nanomachines. Bioessays 2001;23:831–840. [PubMed: 11536295]

Leveque C, Hoshino T, David P, Shoji-Kasai Y, Leys K, Omori A, Lang B, el Far O, Sato K, Martin-Moutot N, Newsom-Davis J, Takahashi M, Seagar MJ. The synaptic vesicle protein synaptotagmin associates with calcium channels and is a putative Lambert-Eaton myasthenic syndrome antigen. Proc Natl Acad Sci USA 1992;89:3625–3629. [PubMed: 1314395]

Lindau M. Time-resolved capacitance measurements: monitoring exocytosis in single cells. Q Rev Biophys 1991;24:75–101. [PubMed: 2047522]

Lindau M, Neher E. Patch-clamp techniques for time-resolved capacitance measurements in single cells. Pfluegers Arch 1988;411:137–146. [PubMed: 3357753]

Maricq AV, Korenbrot JI. Calcium and calcium-dependent chloride currents generate action potentials in solitary cone photoreceptors. Neuron 1988;1:503–515. [PubMed: 2483100]

MacLeish PR, Barnstable CJ, Townes-Anderson E. Use of a monoclonal antibody as a substrate for mature neurons in vitro. Proc Natl Acad Sci USA 1983;80:7014–7018. [PubMed: 6580623]

Mennerick S, Matthews G. Ultrafast exocytosis elicited by calcium current in synaptic terminals of retinal bipolar neurons. Neuron 1996;17:1241–1249. [PubMed: 8982170]

Morgans CW. Localization of the alpha(1F) calcium channel subunit in the rat retina. Invest Ophthalmol Vis Sci 2001;42:2414–2418. [PubMed: 11527958]

Morgans CW, El Far O, Berntson A, Wassle H, Taylor WR. Calcium extrusion from mammalian photoreceptor terminals. J Neurosci 1998;18:2467–2474. [PubMed: 9502807]

Moriondo A, Pelucchi B, Rispoli G. Calcium-activated potassium current clamps the dark potential of vertebrate rods. Eur J Neurosci 2001;14:19–26. [PubMed: 11488945]

Moser T, Beutner D. Kinetics of exocytosis and endocytosis at the cochlear inner hair cell afferent synapse of the mouse. Proc Natl Acad Sci USA 2000;97:883–888. [PubMed: 10639174]

Nachman-Clewner M, St Jules R, Townes-Anderson E. L-type calcium channels in the photoreceptor ribbon synapse: localization and role in plasticity. J Comp Neurol 1999;415:1–16. [PubMed: 10540354]

Neher E. Vesicle pools and Ca^{2+} microdomains: new tools for understanding their roles in neurotransmitter release. Neuron 1998;20:389–399. [PubMed: 9539117]

Neher E, Marty A. Discrete changes of cell membrane capacitance observed under conditions of enhanced secretion in bovine adrenal chromaffin cells. Proc Natl Acad Sci USA 1982;79:6712–6716. [PubMed: 6959149]

Neher E, Zucker RS. Multiple calcium-dependent processes related to secretion in bovine chromaffin cells. Neuron 1993;10:21–30. [PubMed: 8427700]

Neves G, Lagnado L. The kinetics of exocytosis and endocytosis in the synaptic terminal of goldfish retinal bipolar cells. J Physiol 1999;515:181–202. [PubMed: 9925888]

Parsons TD, Lenzi D, Almers W, Roberts WM. Calcium-triggered exocytosis and endocytosis in an isolated presynaptic cell: capacitance measurements in saccular hair cells. Neuron 1994;13:875–883. [PubMed: 7946334]

Poberaj I, Rupnik M, Kreft M, Sikdar SK, Zorec R. Modeling excess retrieval in rat melanotroph membrane capacitance records. Biophys J 2002;82:226–232. [PubMed: 11751311]

Rao-Mirotznik R, Harkins AB, Buchsbaum G, Sterling P. Mammalian rod terminal: architecture of a binary synapse. Neuron 1995;14:561–569. [PubMed: 7695902]

Rapp G, Güth K. A low cost high intensity flash device for photolysis experiments. Pfluegers Arch 1988;411:200–203. [PubMed: 3357758]

Raviola E, Raviola G. Structure of the synaptic membranes in the inner plexiform layer of the retina: a freeze-fracture study in monkeys and rabbits. J Comp Neurol 1982;209:233–248. [PubMed: 7130454]

Rieke F, Schwartz EA. Asynchronous transmitter release: control of exocytosis and endocytosis at the salamander rod synapse. J Physiol 1996;493:1–8. [PubMed: 8735690]

Rouze NC, Schwartz EA. Continuous and transient vesicle cycling at a ribbon synapse. J Neurosci 1998;18:8614–8624. [PubMed: 9786969]

Rupnik M, Kreft M, Sikdar SK, Grilc S, Romih R, Zupancic G, Martin TF, Zorec R. Rapid regulated dense-core vesicle exocytosis requires the CAPS protein. Proc Natl Acad Sci USA 2000;97:5627–5632. [PubMed: 10792045]

Safieddine S, Wenthold RJ. SNARE complex at the ribbon synapses of cochlear hair cells: analysis of synaptic vesicle- and synaptic membrane-associated proteins. Eur J Neurosci 1999;11:803–812. [PubMed: 10103074]

Sakaba T, Tachibana M, Matsui K, Minami N. Two components of transmitter release in retinal bipolar cells: exocytosis and mobilization of synaptic vesicles. Neurosci Res 1997;27:357–370. [PubMed: 9152048]

Schiavo G, Stenbeck G, Rothman JE, Sollner TH. Binding of the synaptic vesicle v-SNARE, synaptotagmin, to the plasma membrane t-SNARE, SNAP-25, can explain docked vesicles at neurotoxin-treated synapses. Proc Natl Acad Sci USA 1997;94:997–1001. [PubMed: 9023371]

Schnapf JL, Copenhagen DR. Differences in the kinetics of rod and cone synaptic transmission. Nature 1982;296:862–864. [PubMed: 6280070]

Sherry DM, Yang H, Standifer KM. Vesicle-associated membrane protein isoforms in the tiger salamander retina. J Comp Neurol 2001;431:424–436. [PubMed: 11223812]

Sugita S, Shin O-H, Han W, Lao Y, Sudhof C. Synaptotagmins form a hierarchy of exocytotic Ca^{2+} sensors with distinct Ca^{2+} affinities. EMBO J 2002;21:270–280. [PubMed: 11823420]

Tachibana M, Okada T, Arimura T, Kobayashi K, Piccolino M. Dihydropyridine-sensitive calcium current mediates neurotransmitter release from bipolar cells of the goldfish retina. J Neurosci 1993;13:2898–2909. [PubMed: 7687280]

Takahashi M, Arimatsu Y, Fujita S, Fujimoto Y, Kondo S, Hama T, Miyamoto E. Protein kinase C and Ca^{2+}/calmodulin-dependent protein kinase II phosphorylate a novel 58-kDa protein in synaptic vesicles. Brain Res 1991;551:279–292. [PubMed: 1655160]

Takahashi N, Kadowaki T, Yazaki Y, Miyashita Y, Kasai H. Multiple exocytotic pathways in pancreatic β cells. J Cell Biol 1997;138:55–64. [PubMed: 9214381]

Thomas P, Wong JG, Lee AK, Almers W. A low affinity Ca^{2+} receptor controls the final steps in peptide secretion from pituitary melanotrophs. Neuron 1993;11:93–104. [PubMed: 8393324]

Tomita T. Retrospective review of retinal circuitry. Vision Res 1986;26:1339–1350. [PubMed: 3303662]

Ubach J, Zhang X, Shao X, Sudhof TC, Rizo J. Ca^{2+} binding to synaptotagmin: how many Ca^{2+} ions bind to the tip of a C2-domain? EMBO J 1998;17:3921–3930. [PubMed: 9670009]

Ullrich B, Sudhof TC. Distribution of synaptic markers in the retina: implications for synaptic vesicle traffic in ribbon synapses. J Physiol 1994;88:249–257.

Voets T. Dissection of three Ca^{2+}-dependent steps leading to secretion in chromaffin cells from mouse adrenal slices. Neuron 2000;28:537–545. [PubMed: 11144362]

Voets T, Moser T, Lund PE, Chow RH, Geppert M, Südhof TC, Neher E. Intracellular calcium dependence of large dense-core vesicle exocytosis in the absence of synaptotagmin I. Proc Natl Acad Sci USA 2001;98:11680–11685. [PubMed: 11562488]

von Gersdorff H. Synaptic ribbons: versatile signal transducers. Neuron 2001;29:7–10. [PubMed: 11182076]

von Gersdorff H, Matthews G. Dynamics of synaptic vesicle fusion and membrane retrieval in synaptic terminals. Nature 1994;367:735–739. [PubMed: 7906397]

von Gersdorff H, Matthews G. Electrophysiology of synaptic vesicle cycling. Annual Rev Physiol 1999;61:725–752. [PubMed: 10099708]

von Gersdorff H, Vardi E, Matthews G, Sterling P. Evidence that vesicles on the synaptic ribbon of retinal bipolar neurons can be rapidly released. Neuron 1996;16:1221–1227. [PubMed: 8663998]

von Kriegstein K, Schmitz F, Link E, Sudhof TC. Distribution of synaptic vesicle proteins in the mammalian retina identifies obligatory and facultative components of ribbon synapses. Eur J Neurosci 1999;11:1335–1348. [PubMed: 10103129]

Xu T, Binz T, Niemann H, Neher E. Multiple kinetic components of exocytosis distinguished by neurotoxin sensitivity. Nat Neurosci 1998;1:192–200. [PubMed: 10195143]

Zenisek D, Steyer JA, Almers W. Transport, capture and exocytosis of single synaptic vesicles at active zones. Nature 2000;406:849–854. [PubMed: 10972279]

Zorec R, Henigman F, Mason WT, Kordas M. Electrophysiological study of hormone secretion by single adenohypophyseal cells. Methods Neurosci 1991;4:194–210.

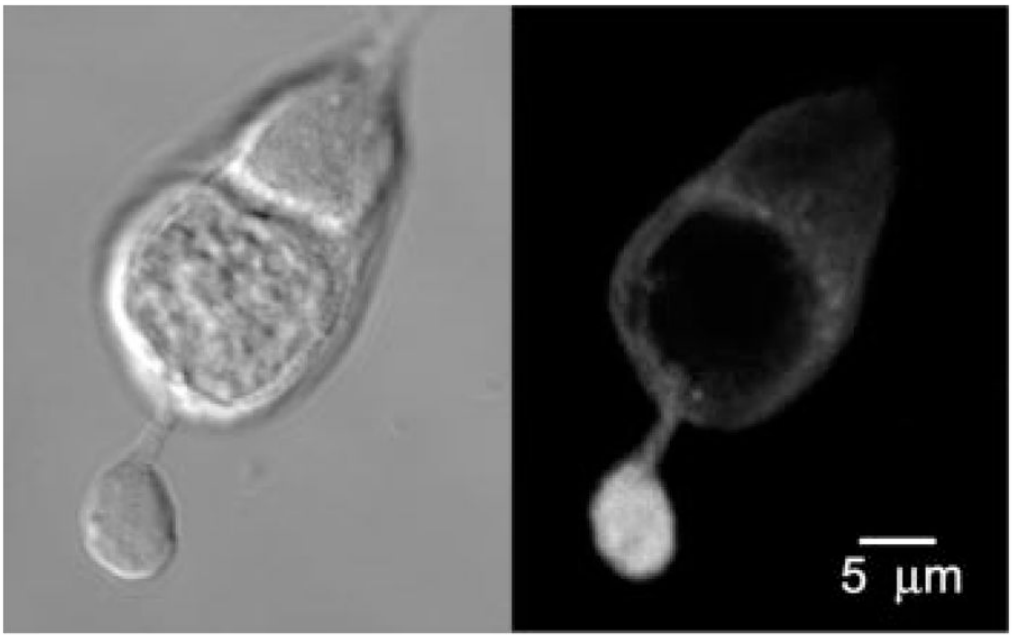

FIG. 1.

Differential interference contrast image of the rod photoreceptor (*left*) and the corresponding confocal immunocytochemical detection of synaptotagmin I (*right*). Note that the synaptotagmin I signal is associated with secretory vesicles in synaptic terminal.

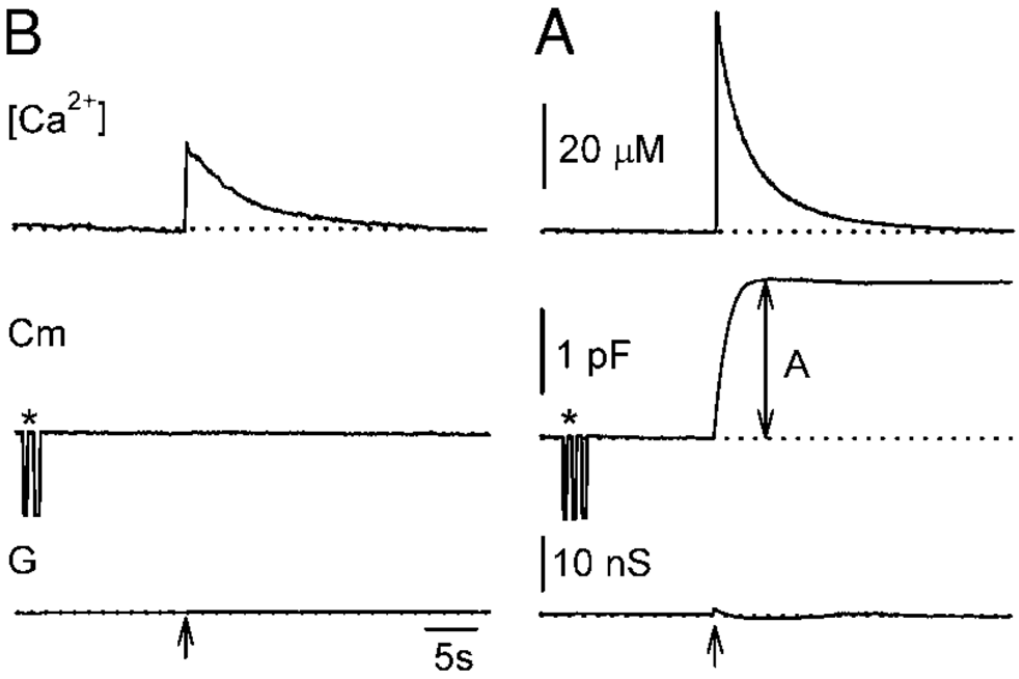

FIG. 2.

Representative time-dependent changes in $[Ca^{2+}]_i$ (top traces), membrane capacitance (C_m, middle traces), and real part of admittance (G, lower traces; reflecting changes in access conductance, membrane conductance, and C_m) after ultraviolet (UV) flash photolysis of Ca^{2+}-loaded NP-EGTA (arrows). The membrane capacitance response is evoked only by high postflash $[Ca^{2+}]_i$ (*B*), but not by the low postflash $[Ca^{2+}]_i$ (*A*). The amplitude of the response in C_m is labeled as *A*. Asterisks are marking 1-pF calibration pulses, used for the determination of the phase angle setting by monitoring the projection of the pulse from the C_m to G output of the lock-in amplifier.

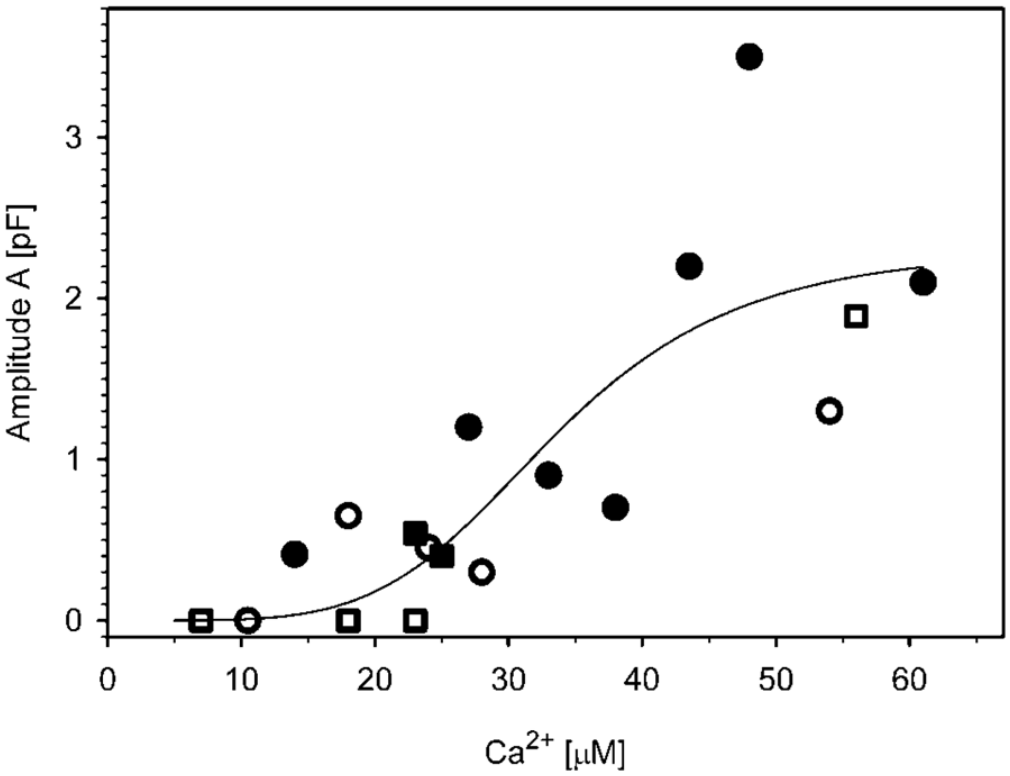

FIG. 3.

Calcium dependence of amplitudes in flash-induced increase in C_m (*A*, see Fig. 2) of exocytic responses in rod (circles) and cone (squares) photoreceptors. The curve represents the best fit to the Hill equation: (pF) = (2.3 ± 0.7)$[Ca^{2+}]^{(4.7\pm2.7)}$/([33.5 ± 7.5 μM]$^{(4.7\pm2.7)}$ + $[Ca^{2+}]^{(4.7\pm2.7)}$), where the parameters are in the format mean ± SE. Filled symbols show cells with double exponential rise in C_m (see Fig. 4).

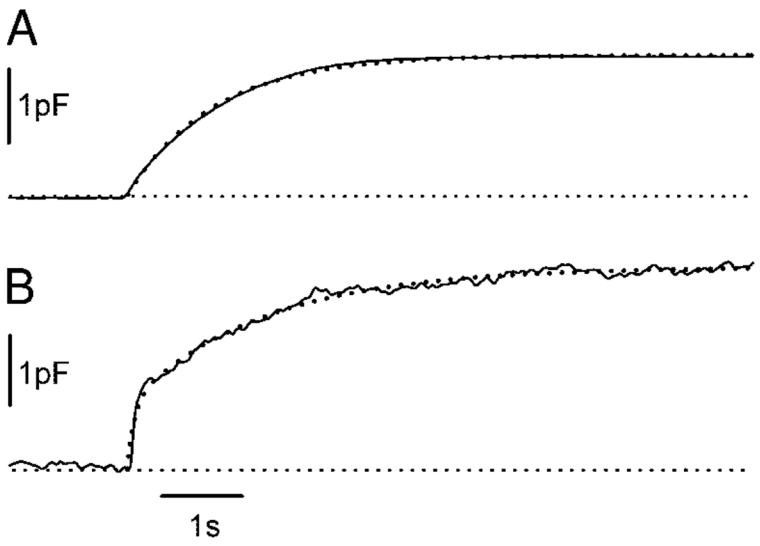

FIG. 4.

Properties of flash-induced C_m responses characterized by a single exponential component (*A*), or a double exponential rise (*B*). Dotted lines represent curves fitted with exponential regression algorithms: (pF) = (1.87 ± 0.0009 pF) * {1 − exp[− (0.839 ± 0.0017 s^{-1}) * *t*]} and (pF) = (0.88 ± 0.035 pF) * {1 − exp[− (10.6 ± 1.45 s^{-1}) * *t*]} + (1.88 ± 0.033 pF) * {1 − exp[− (0.57 ± 0.016 s^{-1}) * *t*]}, where the parameters are in the format mean ± SE. Postflash $[Ca^{2+}]_i$ were 56 μM (*A*) and 61 μM (*B*).

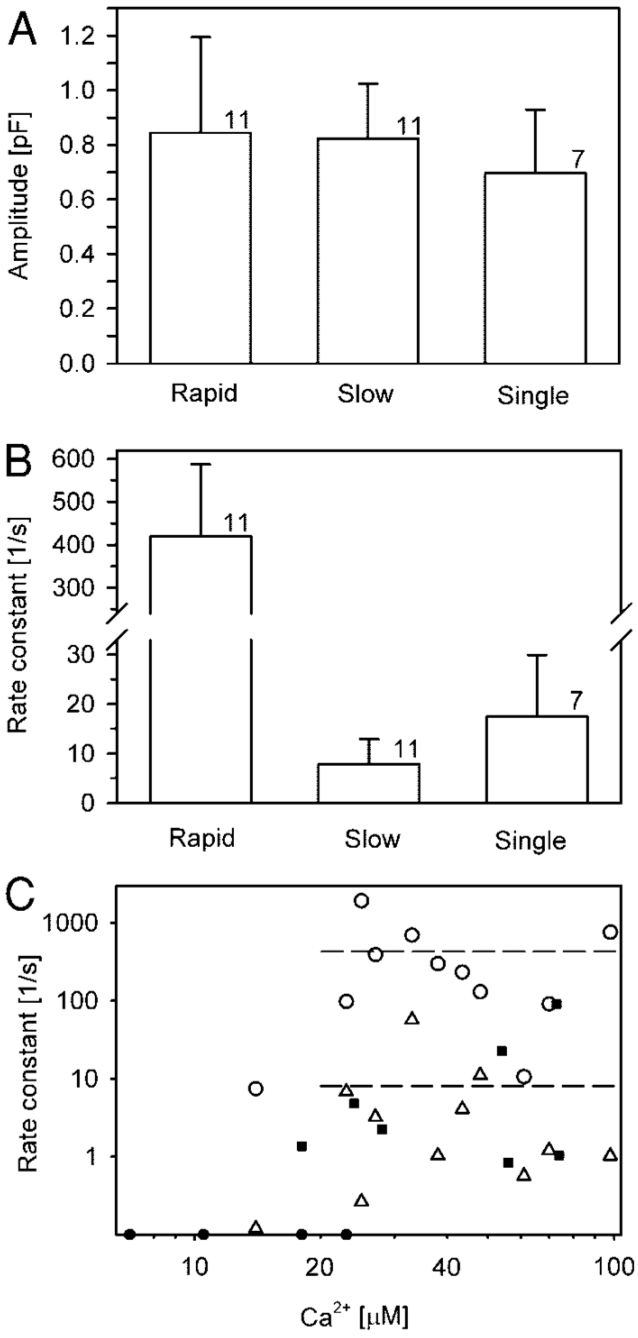

FIG. 5.

A: mean estimated amplitudes of rapid, slow, and single-exponential exocytotic responses obtained by fitting curves to UV flash-induced C_m signals. *B*: mean rate constants of rapid, slow, and single-exponential exocytotic responses elicited by a transient increase in $[Ca^{2+}]_i$. Error bars indicate standard error of the mean. Numbers adjacent to columns indicate numbers of cells studied. Mean postflash $[Ca^{2+}]_i$ in cells with single- and double-exocytotic responses were 46.7 ± 8.8 and 43.7 ± 7.4 μM, respectively (mean ± SE), not significantly different. *C*: relationship between rapid (open circles), slow (open triangles), and single (filled squares) rate constants of vesicle pool depletion and $[Ca^{2+}]_i$ in photoreceptor cells.

Filled circles represent experiments with no exocytic response. Dashed lines represent mean rate constants of rapid and slow exocytic response (420 and 7.85 s^{-1}, respectively).